Predicting Properties and Reactivities of the β-Lactamase Inhibitors Clavulanic Acid, Potassium Clavulanate Salt and its Anion

Silvia Antonia Brandán[*]

Cátedra de Química General, Instituto de Química Inorgánica, Facultad de Bioquímica. Química y Farmacia, Universidad Nacional de Tucumán, Ayacucho 471, (4000) San Miguel de Tucumán, Tucumán, Argentina.

ABSTRACT

The structures and properties of three β-Lactamase inhibitors, clavulanic acid, potassium clavulanate salt and its anion have been theoretically determined in gas phase and in aqueous solution with the hybrid B3LYP/6-31G* calculations. The properties in solution were studied by using the Integral Equation Formalism variant Polarised Continuum Method (IEFPCM) while the solvation energies were predicted with the universal solvation model. The Natural Bond Orbital (NBO) studies have evidenced the high stabilities of anion and of the salt in the two media due to $\Delta E_{\pi \to \sigma*}$, $\Delta E_{n \to \sigma*}$ and $\Delta E_{n \to \pi*}$ transitions while the Atoms in Molecules (AIM) analyses only show high stabilities for the salt. On the other hand, the studies of frontier orbitals and descriptors have suggested higher reactivities of anion in both media. Here, the positive higher nucleophilicity and low electrophilicity indexes values evidenced in the anionic species, in agreement with its mapped MEP surfaces, could clearly support the higher reactivities of anion. Besides, both $f(\nu C=O)$ and $f(\nu O\text{-}H)$ force constants in the anion are in agreement with the higher reactivity and higher solvation energy evidenced by this species. For first time, in this work, the harmonic force fields, scaled force constants and the complete vibrational assignments for the 64 and 60 vibration normal modes expected for the three β-Lactamase inhibitors are respectively reported.

INTRODUCTION

The clavulanic acid and its potassium clavulanate salt, whose chemical structure is (2*R*,3*Z*,5*R*)-3-(2-hydroxyethylidene)-7-oxo-4-oxa-1-azabicyclo [3.2.0] heptane-2-carboxylate, are important β-Lactamase inhibitors used for the treatment of infections caused by beta-lactamase-producing organisms because both species act by blocking the active sites of these enzymes [1-21]. The clavulanic acid is generated by fermentation of *Streptomyces clavuligerus* and together with its salt are widely combined with the antibiotic amoxicillin due to that both species avoid that certain bacteria becoming resistant to it [13,16,18-21]. Hence, during the pharmaceutical preparations of these drugs the control of impurity is a very important factor, for which, there are many analytics methods used to carry out that task being the HPLC technique the official procedure to quality control [22]. However, the infrared technique coupled with attenuated total reflectance (ATR/FTIR) or the Raman spectroscopies are methods highly employed to simultaneous determinations of clavulanic acid and amoxicillin in commercial preparations due to its high versatility [13,14,16,19-21]. Hence, the complete vibrational assignments of all bands observed in the infrared and Raman spectra of clavulanic acid, the potassium clavulanate salt and its anion are important to achieve their identifications in all systems in which they are present. In this senses, the knowledge of their structures in experimental or theoretical forms is also important to explain their biological activities or mechanisms of action and, also, to predict the chemical properties and reactivities of those species derived from clavulanic acid [1-5,14,15]. Theoretical calculations of β-Lactam antibiotics by using AM1 calculations to study the alkaline hydrolysis of clavulanic acid were reported by Frau et al [6] while Miani et al have employed hybrid empirical/quantum mechanical simulations to describe the vibrational levels of clavulanate in solution and, also to simulate its Raman spectrum [14]. Although the experimental structure of potassium clavulanate was already determined by X-ray diffraction [15], so far, the infrared and Raman spectra of clavulanic acid, potassium clavulanate salt and its anion are not completely assigned. Hence, the aims of this work are: (i) the determinations of structures of clavulanic acid, clavulanate salt and its anion in gas phase and in aqueous solution by using theoretical calculations derived from density functional theory (DFT) with the hybrid B3LYP/6-31G* method [23,24], (ii) the determinations of some characteristics properties of those three species by using the same level of theory, (iii) the predictions of reactivities and behaviours of the three species by using the frontier orbitals and finally, (iv) to report the complete assignments of clavulanic acid, clavulanate salt and its anion by using the SQMFF methodology and the

Molvib program [25-27]. Self-consistent reaction field (SCRF) calculations were used to optimize the three species in aqueous solution [28-30]. Here, the predicted properties for these species are compared with the reported for other potassium and sodium salts [31-37].

Mechanical quantum calculations

The *Gauss View* program [38] was used to model the structures of clavulanic acid (CA), potassium clavulanate (PC) salt and its clavulanate anion (AC) in accordance to the geometrical parameters taken from the experimental structure of potassium clavulanate salt from Ref [15]. Here, three stables C1, C2 and C3 structures for CA, the PC salt and its AC anion were studied in both media. All structures differ in the positions of OH groups that belong to the OH-CH$_2$-C=C side chain. Thus, in **Figure 1** are presented the three structures of clavulanic acid while **Figures 2** and **3** shows the three structures for the clavulanate salt and its anion, respectively. Then, in **Figure 4** are given the theoretical C3 structure of salt compared with the experimental determined by X-ray diffraction for the potassium clavulanate salt by Fujii *et al* [15]. The definitions of two rings are also considered in the same figure. Hence, R1 corresponds to five members ring while R2 correspond to four members ring. Posteriorly, the three structures were optimized with the Revision A.02 of Gaussian program in gas phase and in aqueous solution [39]. To a better correlation of calculations in solution, the Integral Equation Formalism variant Polarised Continuum Method (IEFPCM) was employed while the solvation energies of all species were predicted with the universal solvation model [28-30].
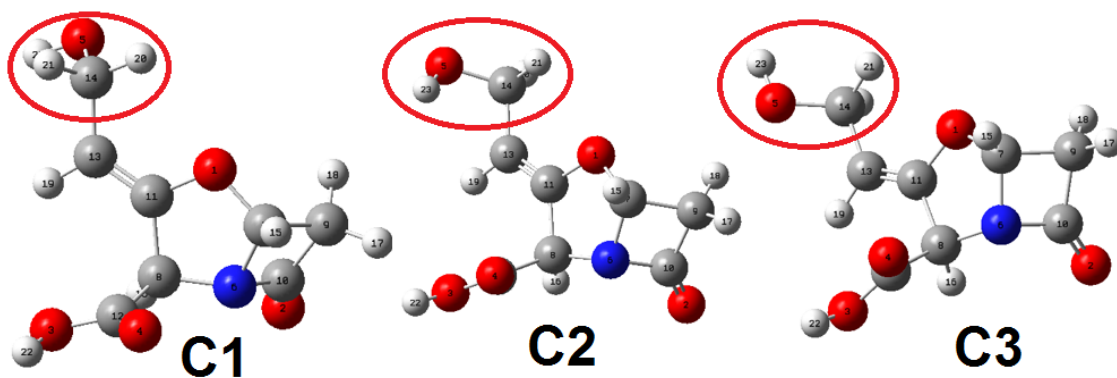

Figure No. 1. Molecular theoretical structures of clavulanic acid showing in red circles the different positions of OH groups.

Citation: Silvia Antonia Brandán. Ijsrm.Human, 2019; Vol. 13 (3): 29-56.

31
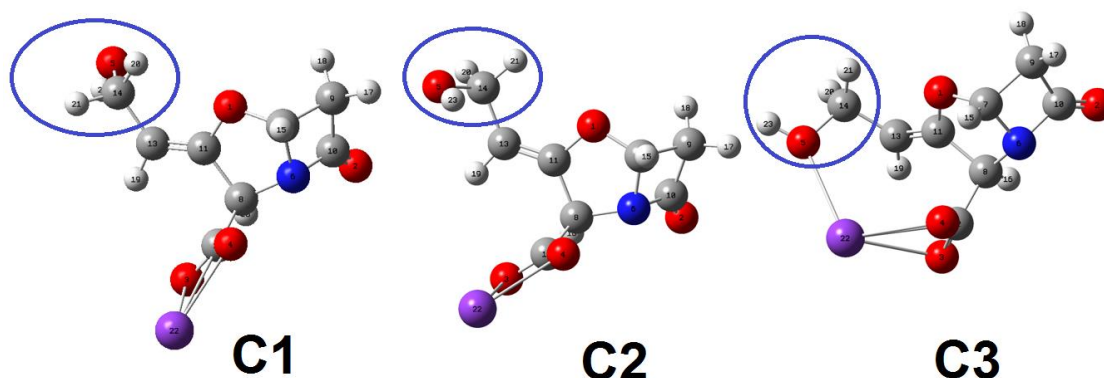
Figure No. 2. Molecular theoretical structures of clavulanate salts showing in blue circles the different positions of OH groups.
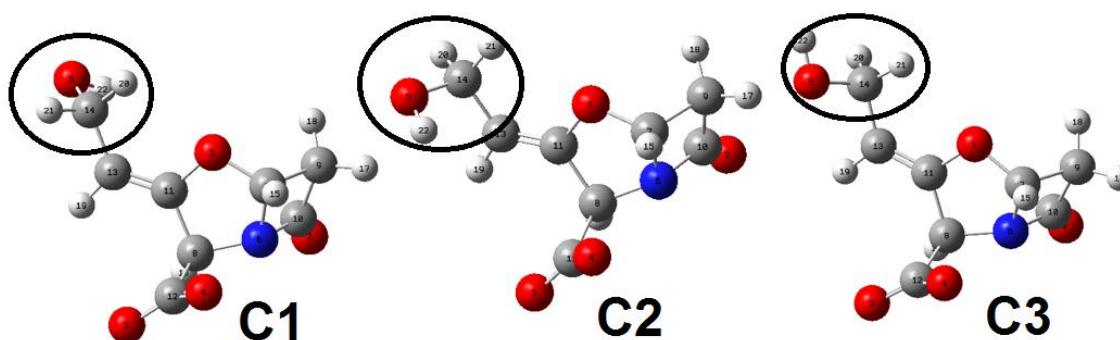
Figure No. 3. Molecular theoretical structures of clavulanate anions showing in black circles the different positions of OH groups.
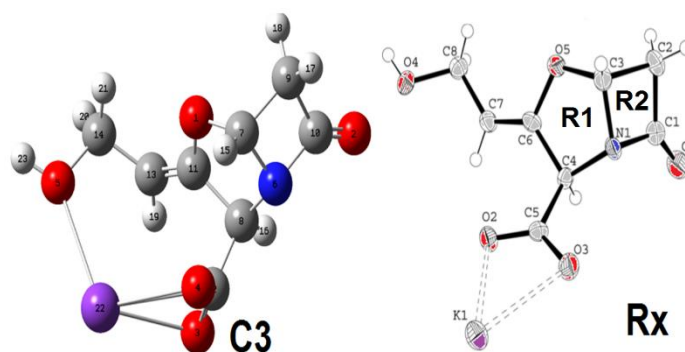
Figure No. 4. Theoretical molecular structure of potassium clavulanate (PC) salt compared with the corresponding experimental taken from Ref [15].

The solvation energies of all species were predicted considering the corrections by Zero Point Vibrational Energy (ZPVE) and computing all volumes in both media with the Moldraw program [40]. The reactivities and behaviours of all species were predicted from the frontier

Citation: Silvia Antonia Brandán. Ijsrm.Human, 2019; Vol. 13 (3): 29-56.

32

orbitals and using some interesting descriptors [31-37] while the harmonic force fields for the three species were calculated with the Scaled Quantum Mechanical Force Field (SQMFF) methodology and the Molvib program by using transferable scaling factors and the corresponding normal internal coordinates for each species. Hence, the harmonic force fields and force constants for all species were obtained applying that methodology [28-30]. To perform the vibrational assignments of bands observed in the available infrared and Raman spectra to the normal vibration modes, only Potential Energy Distribution (PED) contributions major or equal to 10% were considered. Better correlations in the Raman spectra were observed when the theoretical spectra expressed in activities were converted to intensities [41,42].

RESULTS AND DISCUSSION

Structures of all species in both media

Calculated total uncorrected and corrected by ZPVE energies, dipole moments and volumes (V) of three stables C1, C2 and C3 structures of CA, PC and its AC anion were studied in both media. The results are summarized in **Table No. 1**. All calculations were performed by using the B3LYP/6-31G* method.

Citation: Silvia Antonia Brandán. Ijsrm.Human, 2019; Vol. 13 (3): 29-56.

33

Table No. 1. Calculated total energies (*E*), dipole moments (μ) and volumes (V) of clavulanic acid, potassium clavulanate salt and its anion in gas phase and aqueous solution by using the B3LYP/6-31G* method.

Species	E (Hartrees)	ZPVE (Hartrees)	μ (D)	V (Å^3)	ΔE kJ/mol
B3LYP/6-31G* Method					
Gas Phase					
Clavulanic acid					
C1	-741.0812	-740.9074	2.46	187.3	6.03
C2	-741.0837	-740.9097	1.48	192.7	0.00
C3	-741.0810	-740.9074	2.34	189.1	6.03
Potassium Clavulanate salt					
C1	-1340.4555	-1340.2933	11.24	274.0	24.92
C2	-1340.4584	-1340.2960	9.82	276.6	17.84
C3$^{\#}$	-1340.4654	-1340.3028	9.92	255.0	0.00
Clavulanate anion					
C1	-740.5373	-740.3768	8.15	188.8	2.10
C2	-740.5382	-740.3776	7.80	189.3	0.00
C3	-740.5287	-740.3687	9.95	188.2	23.34
Aqueous Solution					
Clavulanic acid					
C1	-741.1122	-740.9387	3.69	188.0	2.10
C2	-741.1130	-740.9394	1.87	192.5	0.00
C3	-741.1111	-740.9379	2.97	189.3	3.93
Potassium Clavulanate salt					
C1	-1340.5042	-1340.3423	13.20	278.3	2.88
C2	-1340.5053	-1340.3434	11.03	272.4	0.00
C3$^{\#}$	-1340.5038	-1340.3421	9.75	267.7	3.41
Clavulanate anion					
C1	-740.6485	-740.4876	10.84	187.5	1.83
C2	-740.6494	-740.4883	12.47	188.3	0.00
C3	-740.6474	-740.4865	14.48	186.1	4.72

[#]Similar to experimental structure according to Ref [15].

Note that for the clavulanic acid and the anion, the most stable forms in gas phase are the C2 ones while the form C3 is the most stable for the clavulanate salt in that medium. In solution, all C2 forms are the most stable for the three species. Evidently, the low ΔE values among the different species in solution could support the presence of all forms in this medium different from the observed in gas phase and in the solid state for the potassium salt because the C3 form is the most stable in these two media. The anionic species present the lower volumes values in both media while the three forms of potassium salt are obviously the most voluminous due to the great size of K^+ cation. In relation to the dipole moment values, the anionic species present higher values, as expected due to that these species are charged in aqueous solution and, as a consequence are most solvated. Hence, it is necessary to know the solvation energies of all species. Therefore, the different solvation energies of all studied forms of CA, PC and its AC anion were predicted, which are the corrected and uncorrected solvation energies by the total non-electrostatic terms and by ZPVE of those three species in the two media by using the B3LYP/6-31G* method. In **Table No. 2** are presented the values for the three species of CA, PC and its AC anion compared with the values reported for potassium 5-hydroxypentanoyl-trifluoroborate (HTFB) [33], potassium 2-isonicotinoyl-trifluoroborate (ITFB) [32], potassium 6-chloro-2-isonicotinoyl-trifluoroborate (Cl-ITFB) [36] and sodium picosulfate salt in aqueous solution [37]. Here, it is clearly observed that the three forms of clavulanate anion have higher solvation energy values than all compared species, having the C3 form anionic the highest value in solution. On the other hand, the sodium picosulfate salt presents higher solvation energy than the three forms of potassium clavulanate salt while the potassium HTFB salt has a higher value (-103.73 kJ/mol) than the observed for the C1 species of potassium clavulanic acid (-101.37 kJ/mol). Besides, the C2 and C3 forms of clavulanic acid show higher solvation energy values than ITFB and Cl-ITFB probably due to their lower molecular weights (199.16 g/mol) in relation to ITFB (212.8 g/mol) and Cl-ITFB (247.3 g/mol). Here, neither the variations of volumes calculated for all salts when they are dissolved in water nor the molecular weights do not justify the solvation energy values because the sodium picosulfate has the highest molecular weight (481.41 g/mol) and high solvation energy (-249.92 kJ/mol). Evidently, other factors have influence on the solvation energy and volume, as probably the characteristics of cations because sodium is different from potassium and the presence of other groups in the structures.

Citation: Silvia Antonia Brandán. Ijsrm.Human, 2019; Vol. 13 (3): 29-56.

35

Table No. 2. Corrected and uncorrected solvation energies by the total non-electrostatic terms and by ZPVE of clavulanic acid, potassium clavulanate salt and its clavulanate anion in aqueous solution by using the B3LYP/6-31G* method.

	B3LYP/6-31G* method[a]				
	Solvation energy (kJ/mol)			MW	ΔV
Species	$\Delta G_{un}^{\#}$	ΔG_{ne}	ΔG_{c}	g/mol	(Å^3)
Clavulanic acid					
C1	-82.10	19.27	-101.37	199.16	0.7
C2	-77.90	19.23	-97.13	199.16	-0.2
C3	-80.00	19.44	-99.44	199.16	0.2
Clavulanate salt					
C1	-128.53	13.63	-142.16	221.14	4.3
C2	-124.33	13.33	-137.66	221.14	-4.2
C3	-103.08	13.50	-116.58	221.14	12.7
Clavulanate anion					
C1	-290.63	18.68	-309.31	182.04	-1.3
C2	-290.36	18.68	-309.04	182.04	-1.0
C3	308.99	18.64	-327.63	182.04	-2.1
HTFB salt[b]	-84.46	19.27	-103.73	207.8	2.8
ITFB salt[c]	-80.96	14.09	-95.05	212.8	22.6
Cl-IFTB salt[d]	-78.69	14.34	-93.03	247.3	0.9
Picosulfate salt[e]	-231.61	18.31	-249.92	481.41	13.3

[a]This work, [b]From Ref [9], [c]From Ref [1], [d]From Ref [3], [e]From Ref [7], $\Delta G_{un}^{\#}$= uncorrected solvation energy, ΔG_{ne}= total non-electrostatic terms, ΔG_{c}= corrected solvation energies

Geometries of all species in both media

In this work, all geometrical parameters for the three forms of CA, PC and its AC anion were calculated in gas phase and in aqueous solution by using the hybrid B3LYP/6-31G* method and then, they were compared with the experimental values determined for the potassium clavulanate salt by Fujii *et al* [2]. The comparisons between experimental and theoretical ones for all species were performed with the Root-Mean-Square Deviation (RMSD) values where the better correlations are observed for the salt, as expected because the experimental data

Citation: Silvia Antonia Brandán. Ijsrm.Human, 2019; Vol. 13 (3): 29-56.

36

correspond to this species. Hence, the theoretical parameters only for the salt in both media are presented in **Table No. 3**. For the three forms of CA, the RMSD values for bond lengths show values between 0.031 and 0.027 Å while for bond angles between 3.6 and 3.0 °. For the anion, the values notably decrease to 0.021-0.010 Å for bond lengths and to 3.9-1.5 ° for bond angles.

Table No. 3. Calculated geometrical parameters of potassium clavulanate salt in gas phase and aqueous solution by using the B3LYP/6-31G* method compared with the corresponding experimental values for this salt taken from Ref [15].

Parameters	B3LYP/6-31G* Method Clavulanate salt						Experimental b
	C1		C2		C3		
	Gas	PCM	Gas	PCM	Gas	PCM	
Bond lengths (Å)							
C7-O1	1.433	1.434	1.434	1.434	1.449	1.434	1.425(5)
C11-O1	1.378	1.387	1.381	1.385	1.366	1.385	1.398(4)
C10=O2	1.203	1.213	1.203	1.213	1.202	1.213	1.199(6)
C12=O4	1.262	1.262	1.263	1.262	1.260	1.262	1.256(59
C12-O3	1.264	1.264	1.263	1.264	1.256	1.264	1.252(5)
C14-O5	1.434	1.442	1.436	1.442	1.464	1.442	1.432(5)
N6-C7	1.459	1.469	1.459	1.470	1.455	1.470	1.480(5)
N6-C8	1.460	1.465	1.460	1.466	1.458	1.466	1.459(5)
N6-C10	1.411	1.406	1.410	1.407	1.412	1.407	1.408(5)
C8-C11	1.535	1.531	1.536	1.532	1.536	1.532	1.522(6)
C8-C12	1.547	1.546	1.546	1.545	1.559	1.546	1.542(5)
C11-C13	1.336	1.336	1.337	1.336	1.343	1.336	1.325(6)
C13-C14	1.501	1.500	1.500	1.498	1.488	1.495	1.485(6)
C7-C9	1.544	1.539	1.544	1.538	1.542	1.538	1.542(5)
C9-C10	1.547	1.528	1.547	1.528	1.548	1.528	1.525(6)
RMSD b	**0.012**	**0.009**	**0.012**	**0.009**	**0.018**	**0.009**	
Bond angles (°)							
O3-C12-O4	126.8	126.4	126.8	126.3	127.9	126.3	125.0(3)
O3-C12-C8	115.8	115.6	115.9	115.7	115.3	115.7	117.7(4)
O4-C12-C8	117.2	117.7	117.1	117.7	115.3	117.7	117.2(3)
C11-O1-C7	109.6	110.1	109.4	110.0	109.4	110.1	109.4(3)
C7-N6-C8	109.5	109.5	109.6	109.6	109.4	109.6	109.9(3)
C8-N6-C10	124.7	122.8	124.6	122.3	125.0	122.4	122.4(4)
C7-N6-C10	92.4	91.0	92.3	90.9	92.3	90.9	91.1(3)
N6-C10-O2	131.3	130.2	131.4	130.2	131.5	130.2	130.1(4)
C9-C10-O2	136.7	136.6	136.7	136.6	136.6	136.6	136.7(4)
C8-C11-	127.2	127.5	127.1	127.2	126.2	127.2	128.8(4)
O1-C11-	122.8	122.8	122.9	122.9	123.2	122.9	121.1(4)

Citation: Silvia Antonia Brandán. Ijsrm.Human, 2019; Vol. 13 (3): 29-56.

37

C11-C13-	125.1	125.3	125.1	125.3	124.6	125.2	127.1(4)
C13-C14-	113.7	112.7	112.3	112.1	107.4	108.5	106.4(3)
RMSD[b]	**2.5**	**2.1**	**2.1**	**1.9**	**1.9**	**1.3**	
			Dihedral angles (º)				
N6-C8-	-154.3	-157.2	-151.0	-	-159.2	-153.4	151.2(4)
N6-C8-	28.0	25.9	32.1	30.4	33.0	30.3	-30.8(6)
C11-C13-	105.5	112.1	-112.9	-	-101.5	-116.9	-137.0(5)
C8-C11-	-179.9	179.7	176.2	176.4	163.0	177.4	179.9(4)
O2-C10-	-52.9	-54.3	-52.3	-54.1	-52.3	-54.1	-53.6(7)

[a]This work, [b]From Ref [15]

Note that the better resuts are observed for the salt, with values of 0.018 and 0.009 for bond lengths and of 2.5 to 1.3 º for bond angles, as observed in Table 3. In all species, the C10=O2 and C11=C13 bonds are predicted with double bond characters in similar form than the C12=O3 and C12=O4 bonds corresponding to the salt and its anion. In these two latter species the absence of cation produce that both C12=O3 and C12=O4 bonds have practically similar values and double bond characters. On the contrary, in the acid, the values of those two bonds are different from the observed in the salt and its anion. On the other hand, the N6-C7 and N6-C8 bonds are predicted with practically the same values but different from the N6-C10 bonds, as was observed experimentally while the C11-O1 bonds are shorter than the C7-O1 bonds. In the salt, the O3-C12-O8 angles are predicted with basically the same values than the O4-C12-O8 angles, as expected because the COOH group is as COO anion in the salt, different from the clavulanic acid. Obviously, in the clavulanate anion are observed double bond characters in the C12=O3, C12=O4 and C11=C13 bonds while enlargement in the C8-C12 bonds are observed in all forms. The three forms of three species show significant differences in the signs of N6-C8-C12-O3 and N6-C8-C12-O4 dihedral angles.

Atomic MK and Mulliken charges and Molecular electrostatic potential (MEP)

The atomic charges are parameters that could explain the properties inhibitors of the species derived from clavulanic acid due to the presence in their structures of different COOH, COO, OH, C=C and C=O groups and of five and four members rings. Hence, the atomic Merz-Kollman (MK) and Mulliken charges on the O and N atoms of clavulanic acid, potassium clavulanate salt and clavulanate anion were calculated in gas phase and in aqueous solution by using the B3LYP/6-31G* method [43]. Thus, in **Table No 4** can be seen the resulted for the most stable species, which are, the C2 forms of clavulanic acid in both media, the C3 and C2

Citation: Silvia Antonia Brandán. Ijsrm.Human, 2019; Vol. 13 (3): 29-56.

38

forms of potassium clavulanate salt in gas phase and in aqueous solution, respectively and the C2 forms of clavulanate anion in both media. For the C2 and C3 conformers of potassium clavulanate salt, only the Mulliken charges were calculated while the MK charges and the Molecular Electrostatic Potentials (MEP) calculated were not obtained probably due to the nature of K cation, as also was observed in the K trifluorobarate salts [31-35]. The variations and behaviours of both charges for the three species in the two media can be easily seen in **Figure No. 5**. The figure shows that the behaviours of both charges in both clavulanic acid and clavulanate anion species are different from the MK charges.

Table No. 4. Atomic MK and Mulliken charges for the most stable conformers of clavulanic acid, potassium clavulanate salt and clavulanate anion in gas phase and aqueous solution by using the B3LYP/6-31G* method.

| Atoms | Clavulonic acid | | Potassium clavulanate salt | | Clavulanate anion | |
| | C2 | | C3 | C2 | C2 | |
	GAS	PCM	GAS	PCM	GAS	PCM
			MK charges[b]			
1 O	-0.286	-0.292			-0.307	-0.314
2 O	-0.475	-0.480			-0.536	-0.531
3 O	-0.585	-0.583			-0.683	-0.706
4 O	-0.478	-0.483			-0.669	-0.685
5 O	-0.651	-0.659			-0.697	-0.695
6 N	-0.551	-0.544			-0.433	-0.469
			Mulliken charges[b]			
1 O	-0.507	-0.510	-0.510	-0.517	-0.531	-0.533
2 O	-0.440	-0.450	-0.452	-0.466	-0.495	-0.495
3 O	-0.562	-0.558	-0.591	-0.625	-0.607	-0.622
4 O	-0.450	-0.456	-0.604	-0.629	-0.611	-0.622
5 O	-0.612	-0.614	-0.653	-0.621	-0.642	-0.633
6 N	-0.414	-0.411	-0.395	-0.404	-0.386	-0.388
			MEP[b]			
1 O	-22.259	-22.259			-22.399	-22.395
2 O	-22.312	-22.314			-22.447	-22.443

Citation: Silvia Antonia Brandán. Ijsrm.Human, 2019; Vol. 13 (3): 29-56.

39

3 O	-22.243	-22.240	-22.556	-22.570
4 O	-22.307	-22.310	-22.554	-22.568
5 O	-22.318	-22.319	-22.439	-22.434
6 N	-18.308	-18.308	-18.451	-18.452

[a]This work, [b]Atomic units (a.u.)

Thus, the MK charges on the O3 and O4 atoms belonging to COO groups show different values in the acid while in the anion both charges together with the charges on O5 atoms are practically constants in both media, as expected due to the absence of K cations in these species. In the acid, the O5 atoms in both media present the most negative values possibly due to that H23 atoms in these species have higher lability and lower values are observed on these atoms. On the other side, the potassium clavulanate salt and its anion present approximately the same behaviours in both media but different values on these charges are observed in both species. In the acid, the Mulliken charges on the O2 and O4 atoms present practically the same values, similar to the MK charges, but the charges observed on N6 in this species in both media are notably higher than the observed on O1, different from the MK charges in the acid where the MK on O1 in both media are higher than the observed on N6. The mulliken charges observed on the O5 atoms of the three species in both media present the most negative values while the N6 atoms have less negative values. The Mulliken charges on the O3 and O4 atoms in the salt and its anion show practically the same values due to the absence of H22 atoms.
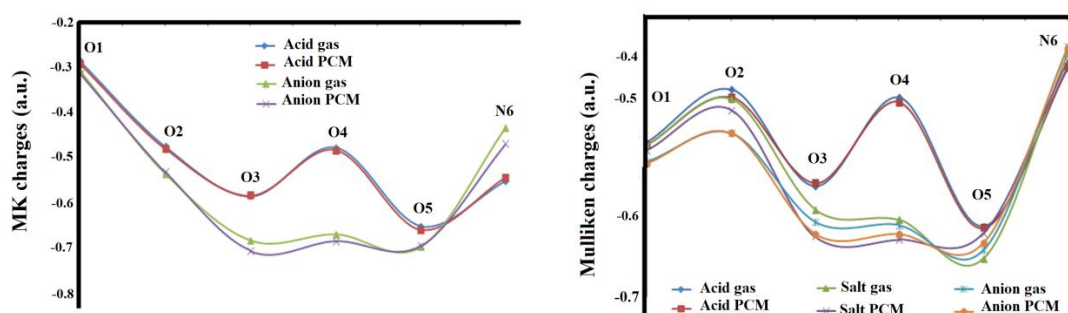

Figure No. 5. Calculated MK and Mulliken charges on O and N atoms of clavulanic acid, potassium clavulanate salt and clavulanate anion in gas phase and aqueous solution by using the B3LYP/6-31G* method.

Citation: Silvia Antonia Brandán. Ijsrm.Human, 2019; Vol. 13 (3): 29-56.

40

The analyses of the MEP from Table 4 show few differences in the values observed on O atoms of acid and anionic species in both media, however, notable differences are observed on the O3 and O4 atoms of both species because the COO groups are protonated in the acid while in the anion are as COO groups. In those two species in both media, the MEP values of N6 are less negative than the O atoms, as expected. Besides, the MEP values in the acid and in the anion do not change when change the medium. When the mapped MEP surfaces are graphed for the most stable conformers of three species in gas phase different colorations are observed in their surfaces, as shown in **Figure No. 6**. Thus, in the acid are observed strong red colours on the O atoms of C=O of the β-lactamase ring and CH$_2$-OH groups and blue colours on the two OH groups. In the salt, the strong red and blue colours are observed respectively on the COO and K groups and, on all suface of anion, it is observed red colour being most strong the coloration on the COO group due to the negative charge on this group.

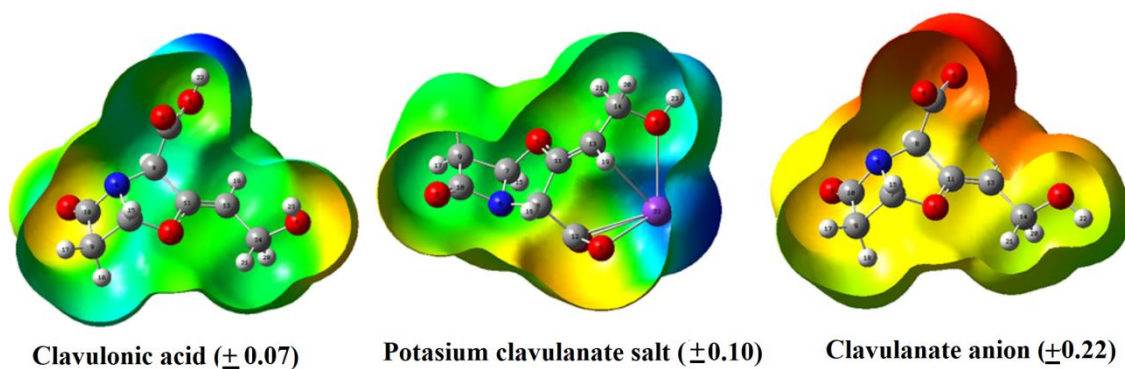Clavulonic acid (± 0.07)   **Potassium clavulanate salt (±0.10)**   Clavulanate anion (±0.22)

Figure No. 6. Calculated electrostatic potential surfaces on the molecular surfaces of clavulanic acid, potassium clavulanate salt and clavulanate anion. Color ranges are indicated in units a.u. B3LYP functional and 6-31G* basis set. Isodensity value of 0.005.

All these different regions and colorations are evidently attributed to the nucleophilic and electrophilic sites where the reaction with biological electrophiles and nucleophiles reactive take places. The green colours in all species are associated to inert regions.

NBO and AIM studies in both media

The stabilization energies and topological analyses for the clavulanic acid, potassium clavulanate salt and clavulanate anion are important studies in these β-Lactamase species taking into account their inhibitors properties. Hence, the Natural Bond Orbital (NBO) and Atoms in Molecules (AIM) programs [44-46] were used to calculate the main delocalization

Citation: Silvia Antonia Brandán. Ijsrm.Human, 2019; Vol. 13 (3): 29-56.

41

energies and topological properties of those three species in gas phase and in aqueous solution by using the B3LYP/6-31G* method. The main delocalization energies for the most stable conformers of three species in both media are presented in **Table No. 5**. Analyzing carefully that table, in the C2 form of CA in solution are observed four different $\Delta ET_{\sigma\to\sigma*}$, $\Delta E_{\pi\to\sigma*}$, $\Delta E_{n\to\sigma*}$ and $\Delta E_{n\to\pi*}$ interactions while in gas phase the $\Delta E_{\sigma\to\sigma*}$ interaction it is not observed for this species. In the C3 conformer of salt in gas phase only are observed the two interactions $\Delta E_{n\to\sigma*}$ and $\Delta E_{n\to\pi*}$ while for the C2 form of salt in solution is also observed the other $\Delta E_{\pi\to\sigma*}$ interaction. Hence, the salt is obviously the most stable species in both media, as compared with the clavulanic acid. If now we analysed the anionic C2 form, three $\Delta E_{\pi\to\sigma*}$, $\Delta E_{n\to\sigma*}$ and $\Delta E_{n\to\pi*}$ interactions are found in the two media where the $\Delta E_{\pi\to\sigma*}$ interactions present lower energy values than the other ones. The total energy favors clearly to the anion in both media with a value of 1426.80 kJ/mol in gas phase while in solution the value decreases to 1343.20 kJ/mol. Probably, the low ΔE_{Total} values observed for the Clavulanic acid indicate that this species in both media are less reactive in the two media.

Table No. 5. Main delocalization energies (in kJ/mol) for clavulanic acid, potassium clavulanate salt and clavulanate anion in gas and aqueous solution phases by using B3LYP/6-31G* calculations.

Delocalization	Clavulonic acid C2		Potassium clavulanate salt C3		Clavulanate anion C2	
	GAS	PCM	GAS	PCM	GAS	PCM
$\sigma C13\text{-}H19\to\sigma*O1\text{-}C11$		42.39				
$\Delta E_{\sigma\to\sigma*}$		42.39				
$\pi O4\text{-}C12\to\sigma*O4\text{-}C12$				105.88	125.90	121.30
$\Delta E_{\pi\to\sigma*}$				105.88	125.90	121.30
$LP(2)O1\to\pi*C11\text{-}C13$	120.55	120.22	143.58	120.97		
$LP(2)O3\to\pi*O4\text{-}C12$	201.69	207.62				
$LP(3)O3\to\pi*O4\text{-}C12$			427.99	333.48		
$LP(3)O4\to\pi*O3\text{-}C12$					524.00	499.89
$LP(1)N6\to\pi*O2\text{-}C10$	132.76	131.63	146.63	141.91	182.46	156.50
$\Delta E_{n\to\pi*}$	455.00	459.47	718.20	596.36	706.46	656.39
$LP(2)O2\to\sigma*N6\text{-}C10$	131.34	125.61	126.24	120.09	115.49	115.16
$LP(2)O2\to\sigma*C9\text{-}C10$	103.58	97.39	106.46	99.07	107.22	101.16
$LP(2)O3\to\sigma*C8\text{-}C12$			86.11	77.37	103.20	88.57

Citation: Silvia Antonia Brandán. Ijsrm.Human, 2019; Vol. 13 (3): 29-56.

42

LP(2)O3→σ*O4-C12			79.04	73.61	84.65	84.27
LP(2)O4→σ*O3-C12	141.87	135.81	74.03	71.48	80.17	82.43
LP(2)O4→σ*C8-C12	90.12	87.24	85.27	81.68	103.71	93.92
$\Delta E_{n \to \sigma*}$	466.91	446.05	557.15	523.30	594.44	565.51
ΔE_{Total}	**921.91**	**947.91**	**1275.35**	**1225.54**	**1426.80**	**1343.20**

Bader's theory was applied in the three β-Lactamase species in order to investigate possible H bonds and intra-molecular interactions by using the topological properties with the AIM2000 program [45,46]. Hence, for the clavulanic acid, potassium clavulanate salt and its clavulanate anion were calculated the electron density, $\rho(r)$, the Laplacian values, $\nabla^2\rho(r)$, the eigenvalues ($\lambda 1$, $\lambda 2$, $\lambda 3$) of the Hessian matrix and, the $|\lambda 1|/\lambda 3$ ratio in the bond critical points (BCPs) and ring critical points (RCPs) by using the B3LYP/6-31G* method. The results for the most stable species are presented in **Table No 6**. Here, we know that if $\lambda 1/\lambda 3 < 1$ and $\nabla^2\rho(r) > 0$ (closed-shell interaction) the interaction is ionic or highly polar covalent when. There are not observed new interactions in the C2 species of CA in both media and only their own RCPs are evidenced. In the C3 species of salt in gas phase, we observed the formation of four ionic interactions with the K$^+$ cation. Thus, the ionic O3-K22, O4-K22, O5-K22 and C13-K22 interactions are formed where, in particular, the first two interactions of K$^+$ cation with the two O atoms of COO group present higher electronic density with approximately the same values. Hence, the distances between both involved atoms are practically the same. The new interactions for all species can be seen in **Figure No 7**.

Table No. 6. Analysis of the Bond Critical Points (BCPs) and Ring critical point (RCPs) of most stable species of clavulanic acid, potassium clavulanate salt and clavulanate anion in gas phase and aqueous solution by using the B3LYP/6-31G* method.

	B3LYP/6-31G* Method[a]					
	Clavulanic acid (C2)					
Parameter[#]	Gas phase				Aqueous solution	
	RCP1	RCP2			RCP1	RCP2
$\rho(r)$	0.0413	0.0908			0.04085	0.0929
$\nabla^2\rho(r)$	0.3151	0.4837			0.3100	0.4862
$\lambda 1$	-0.0457	-0.1316			-0.0453	-0.1359
$\lambda 2$	0.1616	0.2838			0.1596	0.2913
$\lambda 3$	0.1992	0.3315			0.1957	0.3307
$|\lambda 1|/\lambda 3$	0.2294	0.3970			0.2315	0.4109
	Potassium clavulanate salt Gas phase (C3)					

Citation: Silvia Antonia Brandán. Ijsrm.Human, 2019; Vol. 13 (3): 29-56.

43

Parameter[#]	O3-K22	O4-K22	O5-K22	C13-K22	RCPN1	RCPN2	RCPN3	RCP1	RCP2
$\rho(r)$	0.0214	0.0215	0.0146	0.0064	0.0174	0.0058	0.0062	0.0417	0.0916
$\nabla^2\rho(r)$	0.0981	0.0987	0.0636	0.0250	0.0992	0.0224	0.0260	0.3180	0.4878
$\lambda 1$	-0.0206	-0.0206	-0.0143	-0.0042	-0.0134	-0.0021	-0.0041	-0.0464	-0.1318
$\lambda 2$	-0.0175	-0.0178	-0.0129	-0.0025	0.0130	0.0056	0.0045	0.1599	0.2866
$\lambda 3$	0.1361	0.1372	0.0908	0.0314	0.0996	0.0187	0.0256	0.2045	0.3329
$|\lambda 1|/\lambda 3$	0.1514	0.1501	0.1575	0.1338	0.1345	0.1123	0.1602	0.2269	0.3959
Distances (Å)	2.634	2.630	2.781	3.293					

			Potassium clavulanate salt Aqueous solution (C2)						
Parameter[#]	O3-K22	O4-K22		RCPN1				RCP1	RCP2
$\rho(r)$	0.0212	0.0215		0.0152				0.0407	0.0934
$\nabla^2\rho(r)$	0.0886	0.0901		0.0743				0.3092	0.4872
$\lambda 1$	-0.0207	-0.0211		-0.0126				-0.0454	-0.1363
$\lambda 2$	-0.0206	-0.0209		0.0244				0.1581	0.2928
$\lambda 3$	0.1299	0.1321		0.0625				0.1965	0.3306
$|\lambda 1|/\lambda 3$	0.1594	0.1597		0.2016				0.2310	0.4123
Distances (Å)	2.659	2.653							

		Clavulanate anion (C2)				
Parameter[#]	Gas phase				Aqueous solution	
	RCP1	RCP2			RCP1	RCP2
$\rho(r)$	0.0421	0.0924			0.0409	0.0939
$\nabla^2\rho(r)$	0.3216	0.4904			0.3111	0.4891
$\lambda 1$	-0.0458	-0.1318			-0.0453	-0.1357
$\lambda 2$	0.1599	0.2845			0.1580	0.2927
$\lambda 3$	0.2074	0.3375			0.1985	0.3321
$|\lambda 1|/\lambda 3$	0.2208	0.3905			0.2282	0.4086

[a]This work, [#]In a.u. units

The fours ionic interactions generate three new RCPs named RCPN1, RCPN2 and RCPN3, where RCPN1 correspond to ring formed with the COO group, thus, a higher electronic density is observed for this ring critical point. In solution, C2 of salt only present two new ionic interactions formed by the O atoms of COO group with the K^+ cation. The topological properties of these two ionic interactions increase slightly in this media although the electronic densities remain practically in the same value, as observed in Table 6.

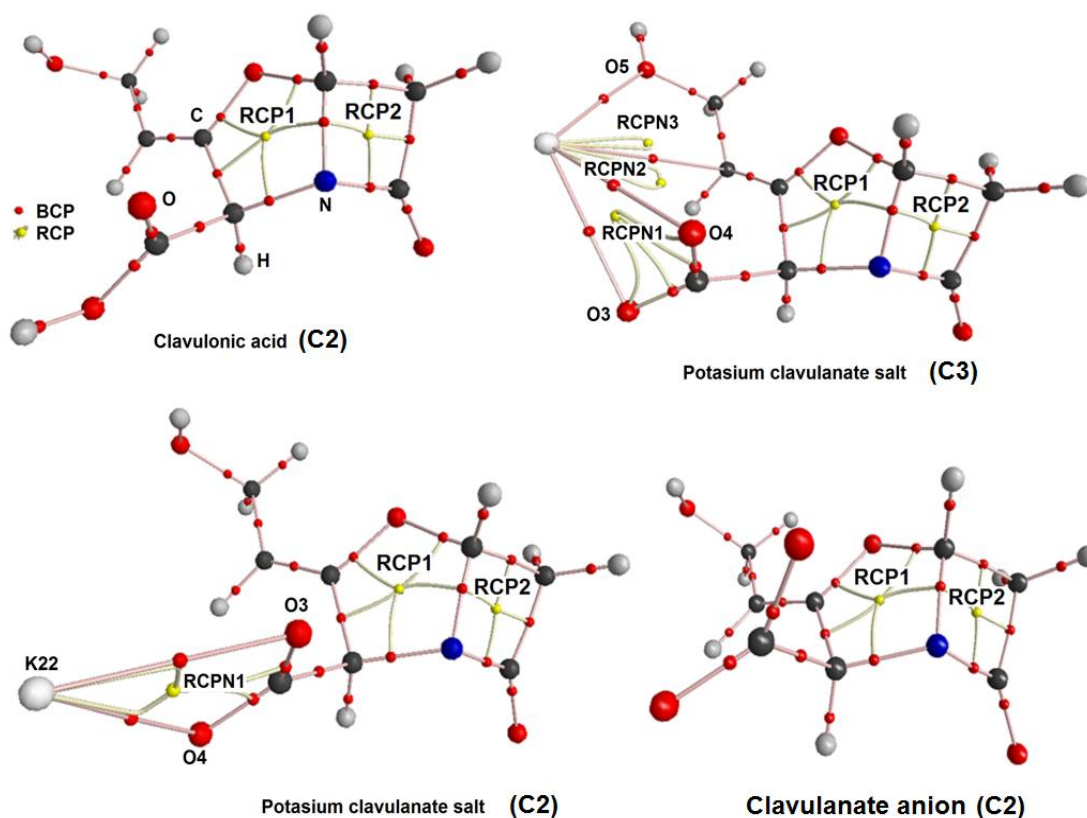*Citation: Silvia Antonia Brandán. Ijsrm.Human, 2019; Vol. 13 (3): 29-56.*

44

Figure No. 7. Molecular graphic for the clavulanic acid, potassium clavulanate salt and its clavulanate anion in gas phase showing the geometry of all their (BCPs) and (RCPs) by using the B3LYP/6-31G* method.

Note that in the anion in both media are not observed new interactions, in similar form than in the acid species. Hence, these studies clearly show the high stability of salt, especially in gas phase due to the four new ionic interactions. Also, the salt evidence a higher stability in solution when it is compared with the acid and anionic species in this medium.

Frontier orbitals and quantum global descriptors studies

The determination of frontier orbitals and of some descriptors, such as the chemical potential (μ), electronegativity (χ), global hardness (η), global softness (S), global electrophilicity index (ω) and global nucleophilicity index (E) are of interest to predict reactivities and behaviours of clavulanic acid, the potassium clavulanate salt and its clavulanate anion in gas phase and aqueous solution. Hence, the gap values were calculated for those species in both media by using the hybrid B3LYP/6-31G* level of theory, as suggested by Parr and Pearson [47] while the descriptors were calculated with known equations and by using the corresponding gap

Citation: Silvia Antonia Brandán. Ijsrm.Human, 2019; Vol. 13 (3): 29-56.

45

values [31-37]. Accordingly, the gap values and the descriptors for CA, PS and AC in both media are shown in **Table No 7**.

Table No. 7. Frontier molecular HOMO and LUMO orbitals, gap values and descriptors (in eV) of clavulanic acid, potassium clavulanate salt and clavulanate anion in gas phase and aqueous solution by using the B3LYP/6-31G* method.

	B3LYP/6-31G* method[a]					
	Clavulonic acid		Potassium clavulanate salt		Clavulanate anion	
Orbitals	C2		C3	C2	C2	
	GAS	PCM	GAS	PCM	GAS	PCM
HOMO	-0.2381	-0.2385	-0.2126	-0.2047	-0.0499	-0.0372
LUMO	-0.021	-0.0224	-0.0417	-0.0602	0.1206	0.1125
$\lvert$GAP$\rvert$	0.2171	0.2161	0.1709	0.1445	0.1705	0.1497
	Descriptors					
Descriptor	C2		C3	C2	C2	
χ	-0.1086	-0.1081	-0.0855	-0.0723	-0.0853	-0.0749
μ	-0.1296	-0.1305	-0.1272	-0.1325	0.0354	0.0377
η	0.1086	0.1081	0.0855	0.0723	0.0853	0.0749
S	4.6062	4.6275	5.8514	6.9204	5.8651	6.6800
ω	0.0773	0.0787	0.0946	0.1214	0.0073	0.0095
E	-0.0141	-0.0141	-0.0109	-0.0096	0.0030	0.0028

[a]This work

$\chi = - [E(LUMO) - E(HOMO)]/2$; $\mu = [E(LUMO) + E(HOMO)]/2$; $\eta = [E(LUMO) - E(HOMO)]/2$; $S = \frac{1}{2}\eta$; $\omega = \mu^2/2\eta$; $E = \mu*\eta$

Analysing the gap values, we observed that the salt and its anion in solution present low gap values and, for these reasons, these species are most reactive than the other ones while the clavulanic acid in both media are the less reactive. Here, the positive higher nucleophilicity values are evidenced by the anionic species, as expected because they are species with negative charges while the salt in solution has the higher electrophilicity value due to K^+ cation. Here, probably the low electrophilicity and high nucleophilicties indexes for the anion could justify its higher reactivities in both media. Besides, the higher solvation energy values observed for the salt and its anion in both media justify clearly their higher reactivities.

Citation: Silvia Antonia Brandán. Ijsrm.Human, 2019; Vol. 13 (3): 29-56.

46

Vibrational study

B3LYP/6-31G* calculations have optimized the clavulanic acid, potassium clavulanate salt and its clavulanate anion in gas phase and in aqueous solution with C_1 symmetries. For the clavulanic acid and the salt are expected 64 normal vibration modes while for the anionic species only 60 modes and, where all modes present activity in both IR and Raman spectra. In **Figure No 8** are compared the experimental available Horizontal Attenuated Total Reflectance (HATR) spectrum of potassium clavulanate salt in the solid phase taken from Ref [48] with the predicted by calculations for the clavulanic acid, potassium clavulanate salt and its clavulanate anion in the gas phase. On the other hand, in **Figure No 9** are compared the experimental available Raman spectrum between 2000 and 400 cm^{-1} taken from Ref [14] with the corresponding predicted for those three species by using the hybrid B3LYP/6-31G* method. The correlations among the experimental and theoretical Raman spectra are notably improved when the predicted spectra in activities are corrected to intensities by using known equations [41,42].
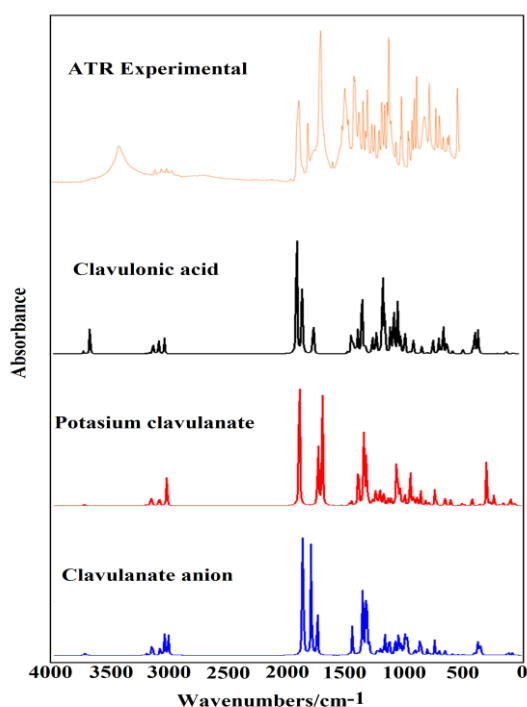

Figure No. 8. Experimental available ATR spectrum of potassium clavulanate salt in solid phase [48] compared with the predicted for clavulanic acid, potassium clavulanate salt and its anion in gas phase and aqueous solution by using the hybrid B3LYP/6-31G* method.
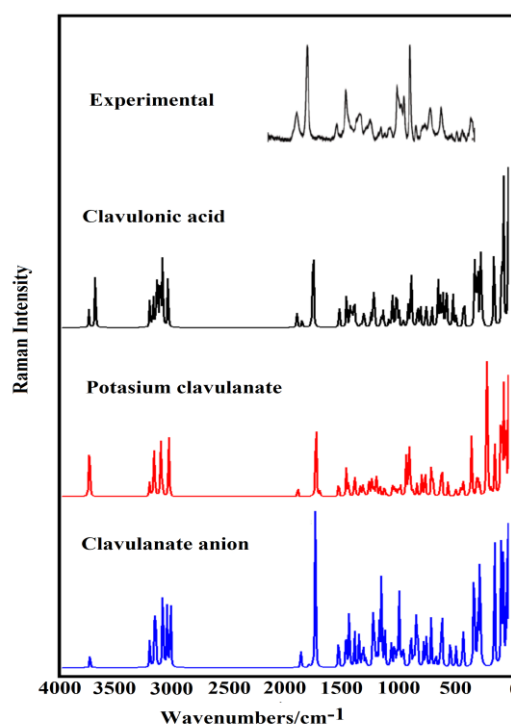
Figure No. 9. Experimental available Raman spectrum of potassium clavulanate salt in solid phase [14] compared with the predicted for clavulanic acid, potassium clavulanate salt and its anion in gas phase and aqueous solution by using the hybrid B3LYP/6-31G* method.

Citation: Silvia Antonia Brandán. Ijsrm.Human, 2019; Vol. 13 (3): 29-56.

47

Both figures show good correlations among the spectra but the better concordances can be seen for the salt, as expected because the spectra presented corresponds to this species. The SQMFF methodology was employed to compute the harmonic force fields for the three species in the two media at the same level of theory taking into account their corresponding normal internal coordinates and the Molvib program [25,27]. The scaling factors were those suggested by Rauhut and Pulay [26] while the potential energy distribution (PED) contributions were calculated with the Molvib program [27] considering PED only major or equal to 10%. The observed and calculated wavenumbers and assignments for the CA, PC salt and its anion are presented in **Table No 8.** The experimental IR bands were taken from available Ref [13] while the experimental ATR and Raman bands were taken from those available from Refs [48,14].

Table No. 8. Observed and calculated wavenumbers (cm^{-1}) and assignments of clavulanic acid, potassium clavulanate salt and its clavulanate anion in gas phase by using the B3LYP/6-31G* method.

B3LYP/6-31G* Method[a]								
Experimental			Clavulonic acid (C2)		Potassium clavulanate salt (C3)		Clavulanate anion (C2)	
IR[c]	ATR[d]	Raman[e]	SQM[b]	Assignments[a]	SQM[b]	Assignments[a]	SQM[b]	Assignments[a]
3405m			3585	νO5-H23	3583	νO5-H23	3571	νO5-H22
3405m	3327w		3528	νO3-H22				
	3075sh		3048	νC13-H19	3048	νC13-H19	3068	νC13-H19
	3075sh		3039	ν_aCH$_2$(C9)	3034	ν_aCH$_2$(C9)	3027	νC7-H15
3015w	3015w		3011	νC7-H15	3005	νC7-H15	3018	ν_aCH$_2$(C9)
3015w	3015w		3008	ν_aCH$_2$(C14)	3004	νC8-H16	3017	νC8-H16
			3001	νC8-H16	3000	ν_aCH$_2$(C14)		
	2960w		2979	ν_sCH$_2$(C9)	2973	ν_sCH$_2$(C9)	2958	ν_sCH$_2$(C9)
2921m	2918w						2922	ν_aCH$_2$(C14)
2858w	2872w		2866	ν_sCH$_2$(C14)	2852	ν_sCH$_2$(C14)	2893	ν_sCH$_2$(C14)
1776s	1776s	1781m	1835	νC10=O2	1819	νC10=O2	1799	νC10=O2
1688m	1700m	1698vs	1788	νC12=O4	1696	νC13=C11	1730	ν_aCOO
1598s	1591vs		1702	νC13=C11	1609	νC12=O4 νC12=O3	1685	νC13=C11
	1473w		1461	δCH$_2$(C14)	1466	δCH$_2$(C14)	1471	δCH$_2$(C14)
1437sh	1406m	1405s	1410	wagCH$_2$(C14)	1411	wagCH$_2$(C14)	1414	wagCH$_2$(C14)
1437sh	1406m	1405s			1406	δCH$_2$(C9)	1409	δCH$_2$(C9)
	1382s	1387sh	1405	δCH$_2$(C9)	1370	νC12=O4 νC12=O3		
1374m	1374sh	1363sh	1374	ρ'C8-H16 ρ'C7-H15	1364	ρ'C7-H15 ρC7-H15	1366	ρ'C7-H15
1350sh	1352m		1359	ρ'C7-H15 ρC7-H15	1317	ρC7-H15 ρC13-H19	1324	ν_sCOO ρ'C7-H15
		1329sh	1329	ρCH$_2$(C14)	1314	ρCH$_2$(C14)	1320	ρC7-H15

Citation: Silvia Antonia Brandán. Ijsrm.Human, 2019; Vol. 13 (3): 29-56.

48

1307sh		1315sh	1316	δO5-H23 ρC7-H15 ρC13-H19	1294	δO5-H23 ρ'C7-H15	1291	ρC13-H19 δO5-H22
1296m	1303s	1292m	1291	ρ'C7-H15	1285	ρ'C8-H16	1282	ν$_s$COO
1263sh	1259m		1274	ρ'C8-H16 δO3-H22			1271	ρ'C8-H16
	1225s	1238sh	1223	ρC8-H16	1216	ρC8-H16		
	1217sh	1216m	1212	wagCH$_2$(C9)	1209	ρC8-H16 ρCH$_2$(C14)	1200	wagCH$_2$(C9)
1200sh	1203w	1195sh	1203	ρCH$_2$(C14) δO5-H23	1206	wagCH$_2$(C9)	1194	ρCH$_2$(C14)
1177w	1187s		1185	νN6-C8	1178	νN6-C8	1170	νN6-C8
1133sh	1147m	1130w	1126	ρCH$_2$(C9)			1152	ρC8-H16
1110w	1123m	1100w	1116	νC12-O3	1118	ρCH$_2$(C9)	1126	νC8-C11 νC11-O1
	1088m	1077sh	1087	νC11-O1 νC8-C11	1097	νC11-O1 νC8-C11	1107	ρCH$_2$(C9)
	1066s	1065w	1059	νN6-C10	1073	νN6-C10	1092	νN6-C7 νN6-C10
1043w	1040s	1049sh	1032	νC13-C14	1033	νC13-C14	1039	νC13-C14
	1014s	1016sh	1030	νC7-O1	1027	νC7-O1	1016	νC7-O1
1008sh	1004vs	1009s	1008	νN6-C7 νC9-C10	1006	νN6-C7 νC9-C10	999	νC9-C10
992m	986m	997sh	981	νC14-O5	971	νC9-C7		
		977m	969	νC9-C7	964	νC14-O5	969	νC14-O5
941sh	942w	953m	925	τwCH$_2$(C14)	933	τwCH$_2$(C14)	957	νC9-C7
	903w	909vs	912	νC8-C12	923	νC8-C12	923	τwCH$_2$(C14)
	895s	897sh			893	νN6-C7 νC11-O1	893	νN6-C7 δC12C8N6
882w			889	νN6-C7 νC11-O1			856	γCOO τwCH$_2$(C14)
878w		862w	874	γC13-H19 τwCH$_2$(C14)	874	γCOO γC13-H19	849	νC8-C12
819w	837m	843vw	838	βR$_2$(A1) νC7-O1	841	βR$_2$(A1) νC7-O1	842	γC13-H19
	805m	808sh	805	γC13-H19	803	γC13-H19	797	γC13-H19 δCOO
	781s	792w			785	δCOO	768	γC13-H19
748w			759	βR$_1$(A2)	732	βR$_1$(A2)	728	δCOO
	765vs	752m	710	γCOO	695	γCOO	690	γCOO
686w	698m		659	βR$_2$(A1)				
637w	656s	668m	649	βR$_1$(A1)	654	βR$_2$(A1)	654	βR$_2$(A1)
622sh	600s	605w	635	δCOO	641	βR$_1$(A1)	641	βR$_1$(A1)
582w	568m	587w	591	γC11-C13	582	γC11-C13	569	γC11-C13
543w	534w	547w	539	τO3-H22				
522sh	500w	505w	522	γC10=O2	523	γC10=O2 τwCH$_2$(C9)	522	γC10=O2 τwCH$_2$(C9)

Citation: Silvia Antonia Brandán. Ijsrm.Human, 2019; Vol. 13 (3): 29-56.

49

488sh		489sh			481	βC10=O2	492	δO5C14C13
	483w		472	βC10=O2	477	δO5C14C13	480	βC10=O2
462sh		460sh	465	δO5C14C13	418	δO1C7C9 ρCOO		
405w	413s	437w	403	δO1C7C9	392	ρCOO	397	δO1C7C9
			363	δO1C7C9	356	δO1C7C9	362	ρCOO, βR2(A1)
			344	ρCOO			348	ρCOO
			253	τO5-H23	290	δO3-K22 δC12C8N6	322	τO5-H22
			234	δC12C8N6	237	τO5-H23	236	δC12C8N6 νC8-C12
					195	νO3-K22		
					179	δC14C13C11 βC11-C13	181	βC11-C13 δC14C13C11
			169	δC14C13C11 βC11-C13	157	δO3-K22 τR2(A1)	160	δC12C8C11
			140	τC13-C11 τR1(A2)	138	δC12C8C11	125	τR1(A1) τR2(A1)
			118	τR2(A1)	114	τC13-C11	114	δC12C8N6 τR1(A2)
			100	τR1(A2)	108	τR1(A2)		
			85	τC13-C11 δC12C8C11	71	τC13-C11 δC12C8N6	79	τC13-C11
			50	τwCOO τC12-C8	48	τR1(A1) τR2(A1)	57	τC14-C13
			45	τC14-C13	45	τwCOO τC12-C8	45	τC13-C11 τR1(A1)
			30	τR1(A1)	27	τC14-C13	41	τwCOO
					23	τO3-K22 δC12C8C11		

Abbreviations: n, stretching; b, deformation in the plane; g, deformation out of plane; wag, wagging; t , torsion; β_R, deformation ring τ_R, torsion ring; ρ, rocking; τw, twisting; δ, deformation; a, antisymmetric; s, symmetric; (A$_1$), Ring 1. [a]This work, [b]From scaled quantum mechanics force field, [c]From Ref [13], [d]From Ref [48], [e]From Ref [14].Some vibration modes are briefly discussed at continuation.

Band Assignments

4000-2000 cm^{-1} region. The antisymmetric and symmetric stretching modes of two CH$_2$ groups, the aromatic C13-H19 and aliphatic C7-H15 and C8-H16 stretching modes and OH stretching modes are expected in this region. Hence, the IR band at 3405 cm^{-1} is assigned to the OH stretching modes, as predicted by calculations while the shoulder in the ATR spectrum at 3075 cm^{-1} is associated to the aromatic C13-H19 stretching mode. The two aliphatic C-H stretching

Citation: Silvia Antonia Brandán. Ijsrm.Human, 2019; Vol. 13 (3): 29-56.

50

modes can be assigned between 3027 and 3001 cm^{-1} because the SQM calculations predicted these modes in that region while the antisymmetric and symmetric CH$_2$ modes are predicted at higher wavenumbers and, for this reason, they are assigned accordingly and in the region expected for other species with similar groups [49-53]. The symmetries of these modes cannot be assigned because there are not bands observed in the Raman spectrum in this 300-2800 cm^{-1} region.

2000-1000 cm^{-1} region. The C10=O2, C12=O3 and C12=O4, C13=C11 stretching modes are characteristic of this region together with the deformation, wagging, rocking modes of CH$_2$ groups, OH deformation, C-H rocking and, C-C and C-N stretching modes. Hence, the intense IR and ATR bands between 1776 and 1598 cm^{-1} can be easily assigned to the C10=O2, C12=O3 and C12=O4, C13=C11 stretching modes, as observed in similar species [49-53], while the strong ATR band and other of medium intensity at 1382 and 1352 cm^{-1} are also assigned to stretching modes of COO group of salt, respectively. In the anion, the symmetric COO modes can be associated to the ATR bands located at 1352 and 1303 cm^{-1}, respectively. The weak Raman band at 1473 cm^{-1} can be assigned to CH$_2$ deformation modes of three species while the strong band in the same spectrum at 1405 cm^{-1} are associated to deformation and wagging modes of those groups of the three species. The rocking modes of CH$_2$ groups in the three species are predicted by calculations between 1329 and 1088 cm^{-1} and, for this reason, they can be assigned in this region, as in similar compounds [49-53]. The SQM calculations predicted the C-H rocking modes between 1374 and 1152 cm^{-1}, therefore, these modes can be associated to the IR, ATR and Raman bands observed in that region. The strong ATR bands between 1187 and 1004 cm^{-1} can be assigned to C-N, C-C and C-O stretching modes because these modes are predicted by SQM calculations in these regions.

1000-10 cm^{-1} region. In this region, the COO in-plane and out-of-plane deformation, rocking and twisting modes, twisting CH$_2$ and deformations and torsions of rings and OH groups are expected, in addition to other modes. The modes predicted by calculations only until 392 cm^{-1} can be assigned because the IR, ATR and Raman spectra were recorded up to 400 cm^{-1}. The description and assignments of all modes observed in this region are detailed in Table 8.

Force Fields

The above studies have evidenced a very important contradiction in the properties predicted for clavulanic acid, potassium clavulanate salt and clavulanate anion in gas phase and in

Citation: Silvia Antonia Brandán. Ijsrm.Human, 2019; Vol. 13 (3): 29-56.

51

aqueous solution because the NBO and AIM studies suggest high stabilities for the salt and its anion in both media. Specifically, for the anion it presents a higher reactivity in aqueous solution with a higher solvation energy value (-327.63 kJ/mol), as expected but, the higher stability together with the higher reactivity for the anion is impossible to understand. Besides, the solvation energy value for the anion (-137.66 kJ/mol) is approximately twice the value of salt while the value of acid is -97.13 kJ/mol. In this context, the force constants of those three β-Lactamase species were here calculated with the idea of explain those strong differences observed. Thus, the harmonic force constants were calculated from their force fields by using the 6-31G* method, the SQMFF methodology [25] and the Molvib program [25]. The scaled force constants for clavulanic acid, potassium clavulanate salt and clavulanate anion in gas phase and in aqueous solution can be seen for the most stable conformers in **Table No 9** compared with some values obtained for the potassium 5-hydroxypentanoyltrifluoroborate salt (HTFB) [31].

Table No. 9. Scaled internal force constants for the clavulanic acid, potassium clavulanate salt and its clavulanate anion in gas phase and aqueous solution by using the B3LYP/6-31G* method.

Force constant	β-Lactamase species[a]						HTFB[b]	
	CA		PC salt		AC			
	Gas	PCM	Gas	PCM	Gas	PCM	Gas	PCM
$f(\nu C{=}O)$	12.86	11.84	11.42	10.69	10.72	9.83	10.3	10.0
$f(\nu O{-}H)$	7.08	7.00	7.79	7.79	7.13	6.31	7.5	7.4
$f(\nu C{-}N)$	4.53	4.46	4.97	4.84	4.66	4.45		
$f(\nu CH_2)$	4.87	4.91	5.29	5.34	4.79	4.88	4.65	4.65
$f(\nu C{-}H)_R$	5.10	5.16	5.63	5.60	5.17	5.16		
$f(\nu C{=}C)$	8.92	8.91	9.24	9.55	8.57	8.73		
$f(\nu C{-}C)$	3.55	3.72	3.92	4.02	3.55	3.75	3.9	3.9
$f(\delta CH_2)$	0.74	0.72	0.83	0.79	0.75	0.74		
$f(\delta OH)$	0.71	0.72	0.80	0.84	0.76	0.80		

Units are mdyn Å^{-1} for stretching and mdyn Å rad^{-2} for angle deformations

[a]This work, [b]From Ref [31]

Analysing first the $f(\nu C{=}O)$ force constants for the three species in both media we observed that for the anion the values are lower than the other ones indicating a strong difference in the

Citation: Silvia Antonia Brandán. Ijsrm.Human, 2019; Vol. 13 (3): 29-56.

52

behaviours of this species. In solution, the $f(\nu O\text{-}H)$ force constant for the anion presents an important decreasing, indicative of a higher hydration of these groups in aqueous solution. Hence, both force constants are in agreement with the higher reactivity and higher solvation energy of anion. The values of those two constants in both media are low for the salt, as compared with the acid, therefore, the higher reactivity and higher solvation energy observed for the salt can also be justified with the $f(\nu C\text{=}O)$ and $f(\nu O\text{-}H)$ force constants. Another important resulted are the different values obtained for the $f(\nu C\text{=}C)$ force constants of the three species in both media. In the salt, the constants present higher values than the other ones showing that in solution the values increase in the salt and its anion. Evidently, the C=C groups play a very important role in the stabilities of three species and, in particular, in aqueous solution. This behaviour in the salt is clearly justified by the new C13-K22 interaction predicted for the acid only in gas phase by using the AIM study. Hence, the salt is most reactive in solution. The other force constants are approximately the same for the three species indicating that practically they have not influence in the properties studied.

CONCLUSIONS

In this work, the structures of three β-Lactamase inhibitors, clavulanic acid, potassium clavulanate salt and its anion have been theoretically determined in gas phase and in aqueous solution with the hybrid B3LYP/6-31G* method. The properties in solution were studied by using the integral equation formalism variant polarised continuum method (IEFPCM) while the solvation energies were predicted with the universal solvation model. The NBO studies have evidenced the high stabilities of anion and of the salt in the two media due to $\Delta E_{\pi \to \sigma*}$, $\Delta E_{n \to \sigma*}$ and $\Delta E_{n \to \pi*}$ interactions while the AIM analyses only show high stabilities for the salt. On the other hand, the studies of frontier orbitals for each species have suggested the higher reactivities of anion in both media. Here, the positive higher nucleophilicity and low electrophilicity indexes values evidenced in the anionic species, in agreement with the strong red colours of its mapped MEP surfaces, could clearly support the higher reactivities of anion. Besides, both $f(\nu C\text{=}O)$ and $f(\nu O\text{-}H)$ force constants are in agreement with the higher reactivity and higher solvation energy evidenced by the anion. In addition, in this work for first time the harmonic force fields, scaled force constants and the complete vibrational assignments for the 64 and 60 vibration normal modes expected for the three β-Lactamase inhibitors are respectively reported.

Citation: Silvia Antonia Brandán. Ijsrm.Human, 2019; Vol. 13 (3): 29-56.

53

Data Availability

The SQM force fields for the three β-Lactamase inhibitors, clavulanic acid, potassium clavulanate salt and its anion can be obtained at request.

Conflicts of Interest

Author declares there is not conflict of interest.

REFERENCES

[1] Charnas RL, Fisher J, Knowles JR. Chemical studies on the inactivation of Escherichia coli RTEM β-lactamase by clavulanic acid, Biochemistry,1978, 17(11): 2185-2189.

[2] Charnas RL, Knowles JR. Inactivation of radiolabeled RTEM .beta.-lactamase from Escherichia coli by clavulanic acid and 9-deoxyclavulanic acid, Biochemistry, 1981, 20(11): 3214–3219.

[3] Boyd DB. Theoretical and Physicochemical Studies on β-Lactam Antibiotics. 1982, 437-545. DOI: 10.1016/B978-0-12-506301-2.50013-7.

[4] Chen CCH, Herzberg O. Inhibition of β-lactamase by clavulanate. Journal of Molecular Biology 1992, 224(4): 1103-1113.

[5] Fernández B, Ríos MA. A Semi-empirical Study of some Clavulanic Acid Derivatives in Relation to their Activity as β-Lactamase Inhibitors. Journal of Pharmacy and Pharmacology, 1993, 45(1): 25-29.

[6] Frau J, Donoso J, Muñoz F, García Blanco F. Theoretical Calculations of β-Lactam Antibiotics. Part VI. AM1 calculations of alkaline hydrolysis of clavulanic acid. Helvetica Chimica Acta, 1994, 77(6): 1557-1569.

[7] Saves I, Burlet-Schiltz O, Swarn P, Lefvre F, Masson JM, Prom JC, Samama JP. The Asparagine to Aspartic Acid Substitution at Position 276 of TEM-35 and TEM-36 Is Involved in the ?-Lactamase Resistance to Clavulanic Acid. Journal of Biological Chemistry 1995, 270(31), 18240-18245.

[8] Miyashita K, Mobashery S. Mechanistic support for the stepwise process for inactivation of class A β-lactamases by clavulanate. Bioorganic & Medicinal Chemistry Letters 1995, 5(10): 1043-1048.

[9] Brown RPA, Aplin RT, Schofield CJ. Inhibition of TEM-2 β-Lactamase from Escherichia coli by Clavulanic Acid: Observation of Intermediates by Electrospray Ionization Mass Spectrometry, Biochemistry 1996, 35(38): 12421-12432.

[10] de la Fuente A, Lorenzana LM, Martín JF, Liras P. Mutants of Streptomyces clavuligerus with Disruptions in Different Genes for Clavulanic Acid Biosynthesis Produce Large Amounts of Holomycin: Possible Cross-Regulation of Two Unrelated Secondary Metabolic Pathways, J. Bacteriology, 2002, 184(2): 6559–65653.

[11] Sulton D, Pagan-Rodriguez D, Zhou X, Liu Y, Hujer AM, Bethel CR, Helfand MS, Thomson JM, Anderson VE, Buynak JD, Ng LM, Bonomo RA. Clavulanic Acid Inactivation of SHV-1 and the Inhibitor-resistant S130G SHV-1?-Lactamase. Journal of Biological Chemistry, 2005, 280(42): 35528-35536.

Citation: Silvia Antonia Brandán. Ijsrm.Human, 2019; Vol. 13 (3): 29-56.

54

[12] Padayatti PS, Helfand MS, Totir MA, Carey MP, Carey PR, Bonomo RA, van den Akker F. High Resolution Crystal Structures of the trans-Enamine Intermediates Formed by Sulbactam and Clavulanic Acid and E166A SHV-1?-Lactamase. Journal of Biological Chemistry 2005, 280(41): 34900-34907.

[13] Ilma N, Sukmadjaja A, Sundani NS, Slamet I. Solid state interaction between amoxicillin trihydrate and potassium clavulanate, Malaysian Journal of Pharmaceutical Sciences, 2007, 5(1): 45–57.

[14] Miani A, Raugei S, Carloni P, Helfand MS. Structure and Raman Spectrum of Clavulanic Acid in Aqueous Solution, J. Phys. Chem. B, 2007, 111(10): 2621–2630.

[15] Fujii K, Toyota K, Sekine A, Uekusa H, Nugrahani I, Asyarie S, Soewandhi NS, Ibrahim S. Potassium clavulanate, Acta Cryst. (2010). E66, m985-m986.

[16] Müller ALH, Flores ÉMM, Müller EI, Silva FEB, Ferrão MF. Attenuated Total Reflectance with Fourier Transform Infrared Spectroscopy (ATR/FTIR) and Different PLS Algorithms for Simultaneous Determination of Clavulanic Acid and Amoxicillin in Powder Pharmaceutical Formulation, J. Braz. Chem. Soc., 2011, 22(10): 1903-1912.

[17] Power P, Mercuri P, Herman R, Kerff G, Gutkind F, Dive G, Galleni M, Charlier P, Sauvage E. Novel fragments of clavulanate observed in the structure of the class A -lactamase from Bacillus licheniformis BS3. Journal of Antimicrobial Chemotherapy 2012, 67(10):, 2379-2387.

[18] Singh ANK, Sekar M, Viswanath V, Reza H. formulation development and evaluavation of amoxicillin trihydrate and potassium clavulanate immediate release tablets, International Journal of Universal Pharmacy and Bio Sciences, 2013, 2(6): 71-87.

[19] Chong XM, Zou WB, Yao SC, Hu CQ. Rapid Analysis of the Quality of Amoxicillin and Clavulanate Potassium Tablets Using Diffuse Reflectance Near-Infrared Spectroscopy, AAPS PharmSciTech., 2017, 18(4): 1311-1317.

[20] Zou WB, Chong XM, Wang Y, Hu CQ. Compilation of a Near-Infrared Library for Construction of Quantitative Models of Oral Dosage Forms for Amoxicillin and Potassium Clavulanate, Frontier in Chem. 2018, 6: 184.

[21] Zou W-b, Chong X-m, Wang Y, Hu, C-q. Compilation of a Near-Infrared Library for Construction of Quantitative Models of Oral Dosage Forms for Amoxicillin and Potassium Clavulanate, Frontier in Chemistry, 6, 184 (2018) 1-12.

[22] The United States Pharmacopeia Convention, The Official Compendia of Standards, USP 33-NF 26, Rockville, 2008.

[23] Lee C, Yang W, Parr RG. Development of the Colle-Salvetti correlation-energy formula into a functional of the electron density. Phys. Rev., 1988, B37: 785-789.

[24] Becke AD. Density-functional exchange-energy approximation with correct asymptotic behavior. Phys. Rev., 1988, A38: 3098-3100.

[25] Pulay P; Fogarasi G; Pongor G, Boggs JE; Vargha A. Combination of theoretical ab initio and experimental information to obtain reliable harmonic force constants. Scaled quantum mechanical (QM) force fields for glyoxal, acrolein, butadiene, formaldehyde, and ethylene. J. Am. Chem. Soc.,1983, 105: 7073.

[26] a) Rauhut G, Pulay P, Transferable Scaling Factors for Density Functional Derived Vibrational Force Fields. J. Phys. Chem., 1995, 99: 3093-3100. b) *Correction:* Rauhut G, Pulay P. J. Phys. Chem., 1995, 99: 14572.

[27] Sundius T. Scaling of ab-initio force fields by MOLVIB. Vib. Spectrosc., 2002, 29: 89-95.

[28] Miertus S, Scrocco E, Tomasi J. Electrostatic interaction of a solute with a continuum. Chem. Phys, 1981, 55: 117–129.

[29] Tomasi J, Persico J. Molecular Interactions in Solution: An Overview of Methods Based on Continous Distributions of the Solvent. Chem. Rev., 1994, 94: 2027-2094.

[30] Marenich AV, Cramer CJ, Truhlar DG. Universal solvation model based on solute electron density and a continuum model of the solvent defined by the bulk dielectric constant and atomic surface tensions. J. Phys. Chem., 2009, B113: 6378-6396.

[31] Iramain MA, Davies L, Brandán SA. FTIR, FT-Raman and UV-visible spectra of Potassium 3-furoyltrifluoroborate, J. Mol. Struc. 2018, 1158: 245-254.

[32] Iramain MA, Davies L, Brandán SA. Evaluating structures, properties and vibrational and electronic spectra of the potassium 2-isonicotinoyltrifluoroborate salt, J. Mol. Struct. 2018, 1163: 41-53.

Citation: Silvia Antonia Brandán. Ijsrm.Human, 2019; Vol. 13 (3): 29-56.

55

[33] Iramain MA, Davies L, Brandán SA. Structural and spectroscopic differences among the potassium 5-hydroxypentanoyltrifluoroborate salt and the furoyl and isonicotinoyl salts, J. Mol. Struct. 2019, 1176: 718-728.

[34] Iramain MA, Ledesma AE, Brandán SA. Structural properties and vibrational analysis of Potassium 5-Br-2-isonicotinoyltrifluoroborate salt. Effect of Br on the isonicotinoyl ring, J Mol. Struct. 2019, 1184: 146-156.

[35] Iramain MA, Brandán SA. Impact of Br on the isonicotinoyl ring and its effects on the properties of Potassium 5-Br-2-isonicotinoyltrifluoroborate salt in different media, submitted to J. Molecular Modeling (2018).

[36] Iramain MA, Brandán SA. Role of Halogen F---H Bonds in Potassium Trifluoroborate Salts, International Journal of Current Advanced Research, 2019, 8(6A): 18527-18529.

[37] Romani D, Salas Tonello I, Brandán SA. Influence of atomic bonds on the properties of the laxative drug sodium picosulphate, Heliyon, 2016, 2: e00190.

[38] Nielsen AB, Holder AJ. Gauss View 3.0. User's Reference, GAUSSIAN Inc., Pittsburgh, PA, 2000–2003.

[39] Frisch MJ, Trucks GW, Schlegel HB, Scuseria GE, Robb MA, Cheeseman JR, Scalmani G, Barone V, Mennucci B, Petersson GA, Nakatsuji H, Caricato M, Li X, Hratchian HP, Izmaylov AF, Bloino J, Zheng G, Sonnenberg JL, Hada M, Ehara M, Toyota K, Fukuda R, Hasegawa J, Ishida M, Nakajima T, Honda Y, Kitao O, Nakai H, Vreven T, Montgomery JA, Peralta JE, Ogliaro F, Bearpark M, Heyd JJ, Brothers E, Kudin KN, Staroverov VN, Kobayashi R, Normand J, Raghavachari K, Rendell A, Burant JC, Iyengar SS, Tomasi J, Cossi M, Rega N, Millam JM, Klene M, Knox JE,. Cross JB, Bakken V, Adamo C, Jaramillo J, Gomperts R, Stratmann RE, Yazyev O, Austin AJ, Cammi R, Pomelli C, Ochterski JW, Martin RL, Morokuma K, Zakrzewski VG, Voth GA, Salvador P, Dannenberg JJ, Dapprich S, Daniels AD, Farkas O, Foresman JB, Ortiz J., Cioslowski J, Fox DJ. Gaussian, Inc., Wallingford CT, 2009.

[40] Ugliengo P. Moldraw Program, University of Torino, Dipartimento Chimica IFM, Torino, Italy, 1998.

[41] Keresztury G, Holly S, Besenyei G, Varga J, Wang AY, Durig JR. Vibrational spectra of monothiocarbamates-II. IR and Raman spectra, vibrational assignment, conformational analysis and ab initio calculations of S-methyl-N,N-dimethylthiocarbamate. Spectrochim. Acta, 1993, 49A: 2007-2026.

[42] Michalska D, Wysokinski. The prediction of Raman spectra of platinum(II) anticancer drugs by density functional theory. Chemical Physics Letters, 2005, 403: 211-217.

[43] Besler BH, Merz Jr KM, Kollman PA. Atomic charges derived from semiempirical methods. J. Comp. Chem., 1990, 11: 431-439.

[44] Glendening E, Badenhoop JK, Reed AD, Carpenter JE, Weinhold F. NBO 3.1; Theoretical Chemistry Institute, University of Wisconsin; Madison, WI, 1996.

[45] Bader RFW. Atoms in Molecules, A Quantum Theory, Oxford University Press, Oxford, 1990, ISBN: 0198558651.

[46] Biegler-Köning F, Schönbohm J, Bayles D. AIM2000; A Program to Analyze and Visualize Atoms in Molecules. J. Comput. Chem., 2001,22: 545.

[47] Paar RG, Pearson RG. Absolute hardness: companion parameter to absolute electronegativity. J. Am. Chem. Soc., 1983, 105: 7512-7516.

[48] https://spectrabase.com/spectrum/

[49] Romani D, Brandán SA, Márquez MJ, Márquez MB. Structural, topological and vibrational properties of an isothiazole derivatives series with antiviral activities. J. Mol. Struct., 2015, 1100: 279-289.

[50] Chain F, Ladetto MF, Grau A, Catalán CAN, Brandán SA. Structural, electronic, topological and vibrational properties of a series of N-benzylamides derived from Maca (*Lepidium meyenii*) combining spectroscopic studies with ONION calculations. J. Mol. Struct. 2016, 1105: 403-414.

[51] Romano E, Castillo MV, Pergomet JL, Zinczuk J, Brandán SA. Synthesis, structural and vibrational analysis of (5,7-Dichloro-quinolin-8-yloxy) acetic acid. J. Mol. Struct., 2012, 1018: 149–155.

[52] Issaoui N, Ghalla H, Brandán SA, Bardak F, Flakus HT, Atac A, Oujia B. Experimental FTIR and FT-Raman and theoretical studies on the molecular structures of monomer and dimer of 3-thiopheneacrylic acid. J. Mol. Struct., 2017, 1135: 209-221.

[53] Minteguiaga M, Dellacassa E, Iramain MA, Catalán CAN, Brandán SA. FT-IR, FT-Raman, UV-Vis, NMR and structural studies of Carquejyl Acetate, a component of the essential oil from *Baccharis trimera* (Less.) DC. (Asteraceae). J Mol. Struct. 2018, 1177: 499-510.

Citation: Silvia Antonia Brandán. Ijsrm.Human, 2019; Vol. 13 (3): 29-56.

56